Zinc(II) Oxide Stability in Alkaline Sodium Phosphate Solutions at Elevated Temperatures

Stephen E. Ziemniak* and Edward P. Opalka

Knolls Atomic Power Laboratory, P.O. Box 1072, Schenectady, New York 12301-1072

Received November 5, 1993. Revised Manuscript Received January 19, 1994®

Zinc oxide (ZnO) is shown to transform into either of two phosphate-containing compounds in relatively dilute alkaline sodium phosphate solutions at elevated temperatures via $ZnO(s) + Na^+ + H_2PO_4^- \rightleftarrows NaZnPO_4(s) + H_2O$ or $2ZnO(s) + H_3PO_4(aq) \rightleftarrows Zn_2(OH)PO_4(s) + H_2O$. X-ray diffraction analyses indicate that $NaZnPO_4$ possesses an orthorhombic unit cell having lattice parameters $a = 8.710 \pm 0.013$, $b = 15.175 \pm 0.010$, and $c = 8.027 \pm 0.004$ Å. The thermodynamic equilibria for these reactions were defined in the system $ZnO-Na_2O-P_2O_5-H_2O$ for Na/P molar ratios between 2.1 and 3. On the basis of observed reaction threshold values for sodium phosphate concentration and temperature, the standard entropy ($S°$) and free energy of formation ($\Delta G_f°$) for $NaZnPO_4$ were calculated to be 169.0 J/(mol K) and −1510.6 kJ/mol, respectively; similar values for $Zn_2(OH)PO_4$ (tarbuttite) were 235.9 J/(mol K) and −1604.6 kJ/mol. Additions of sodium sulfite and sulfate did not alter the above reactions.

Introduction

Recent investigation of the solubility/phase behavior of zinc(II) oxide in alkaline sodium phosphate solutions[1] established a $ZnO/NaZnPO_4$ phase boundary in terms of an equilibrium constant for the liquid-phase composition: $[Na^+][H_2PO_4^-]$. According to Thilo and Schulz,[2] precipitation of a second basic salt of zinc(II) oxide, $Zn_2(OH)PO_4$ (tarbuttite), is possible under mildly alkaline, hydrothermal conditions. A hydrous form of this mineral is also known to exist: $Zn_2(OH)PO_4 \cdot 1.5H_2O$ (spencerite).

The present work was undertaken to determine (a) the manner in which sulfur oxyanion salts (sulfate and sulfite) affect formation of $NaZnPO_4$ and (b) whether a sodium-free zinc phosphate compound would form in the system $ZnO-Na_2O-P_2O_5-H_2O$ for $2 < Na/P < 3$.

Experimental Section

Autoclave Tests. All tests were conducted in a 1-L, gold-lined autoclave vessel fitted with a platinum dip tube to permit hot sampling. A sketch of the apparatus is shown in Figure 1. The experimental methodology was the same as that described previously,[3] viz., incrementally elevate the temperature of a sodium phosphate solution in contact with a ZnO powder reactant until a phosphate loss is observed.

Reagents. Demineralized and deaerated water (resistivity >1 MΩ-cm) was used to prepare all test solutions used in our experiments. All chemicals used [ZnO, Na_2HPO_4 (anhydrous), $Na_3PO_4 \cdot 12H_2O$, Na_2SO_3, and Na_2SO_4 (anhydrous)] were of analytical or equivalent grade obtained from Fisher Scientific Co. or the GSA Chemical Commodities Agency. Zinc oxide was tested in its as-received condition.

Analytical Procedures. The total phosphate concentration and sodium-to-phosphate molar ratio (Na/P) of each sample aliquot were determined by the potentiometric titration procedure described previously.[3] The existence of lower phosphate concentrations, however, made it prudent to titrate larger aliquots (up to 50 g of solution) in order to achieve the stated accuracies.

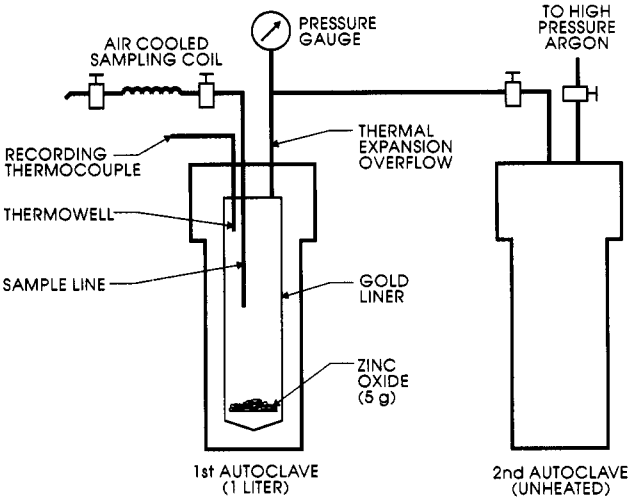

Figure 1. Schematic of autoclave arrangement used in zinc oxide transformation study.

The above procedure was modified for sulfite determination (in the presence of phosphate), based on the reaction with formaldehyde:

$$SO_3^{2-} + CH_2O + H_2O \rightleftarrows (CH_2OH)(SO_3^-) + OH^- \quad (1)$$

After titrating to the first phosphate hydrolysis point at pH = 9.2 ± 0.1, sufficient formaldehyde was added to the liquid sample to react completely with the sulfite. The hydroxyl ions thus liberated increased the solution pH, which was then titrated back to the original pH = 9.2 ± 0.1 value. The equivalent amount of titrant used was equal to the amount of sulfite present. The expected accuracy of this procedure is ±3%. Sulfate ion concentrations were determined by ion chromatographic analysis with an accuracy of ±10%.

Upon completion of each autoclave experiment, the reacted zinc oxide powder was rinsed with deionized water to remove any traces of unreacted sodium phosphate and subjected to visual examination under a stereomicroscope. A portion of the reaction cake was then fractured and placed on a mount for high magnification viewing on a scanning electron microscope. By means of micromanipulators, i.e., needles and tweezers, the reaction product crystals were separated from the remaining mass of unreacted/reacted material. Samples isolated in this manner were subjected to X-ray diffraction (XRD) analyses. Powder

* To whom correspondence should be addressed.

® Abstract published in *Advance ACS Abstracts,* March 1, 1994.

(1) Ziemniak, S. E.; Jones, M. E.; Combs, K. E. S. *J. Solut. Chem.* **1992**, *24*, 1153.
(2) Thilo, E.; Schulz, I. *Z. Anorg. Allg. Chem.* **1951**, *265*, 14.
(3) Ziemniak, S. E.; Opalka, E. P. *Chem. Mater.* **1993**, *5*, 690.

0897-4756/94/2806-0461$04.50/0

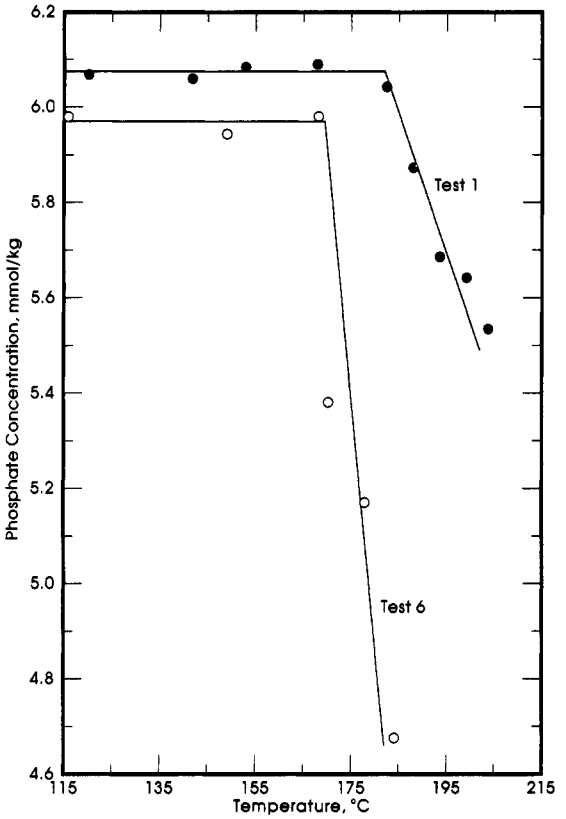

Figure 2. Phosphate variations caused by heating in the presence of zinc(II) oxide.

XRD measurements were performed using a Model CN2155D5 Rigaku diffractometer (Bragg-Brentano geometry) and Cu Kα radiation (λ = 1.5417 Å). The X-ray tube was operated at 45 kV and 20 ma. Data were taken as a continuous scan from 8 to 92° (2θ) at a speed of 1°/min.

In an attempt to react to completion, test 4 was charged with 2 g of ZnO, rather than 5 g, and operated for 7 days. The reaction product from this test was subjected to additional characterizations by infrared spectroscopy (IR) and quantitative chemical analyses. The solids IR spectrum was obtained on a Perkin-Elmer Model 283 spectrometer using the KBr pellet technique. Elemental chemical microanalyses were performed by Galbraith Laboratories, Inc. (Knoxville, TN).

Results

Zinc Oxide Phase Boundary I. Threshold temperatures at which sodium phosphate precipitation was initiated, were determined by reverse extrapolation of phosphate concentration versus temperature plots. At least three temperature points above the threshold levels were included from each run. This process is illustrated in Figure 2. On the basis of changes in the Na/P ratios of the depleted test solutions, compared with initial (baseline) values, indicated Na/P loss ratios were calculated. These values, along with the estimated ZnO transformation temperatures, are summarized in Table 1. No losses of any sulfur oxyanion species (sulfate or sulfite) were observed.

The above results indicate that the zinc oxide–sodium phosphate reaction product from all eight tests contained sodium and phosphate in a 1:1 molar ratio. Test 4, which decomposed the entire 0.025 mol charge of ZnO, precipitated approximately 0.026 mol of phosphate from solution. This result indicates a reaction product composition Zn/P $\approx$ 1.

Table 1. Zinc(II) Oxide Phase Transformation Thresholds

	baseline		threshold	final		indicated Na/P
test	phosphate[a]	Na/P[b]	temp, K	phosphate[a]	Na/P[b]	loss
1	6.076	2.159	455	3.928	2.775	1.0
2	6.507	2.513	482	3.980	3.748	0.6
3	6.339	2.781	472	3.433	4.260	1.0
4	111.6	2.166	353	85.29	2.540	1.0
5	6.223	2.158 (1)	400	4.349	2.623	1.1
6	5.970	2.458 (2)	443	4.675	2.887	0.9
7	6.781	2.202 (3)	439	5.212	3.300	[c]
8	5.517	2.452 (4)	455	3.780	3.153	0.9

[a] mmol/kg. [b] Na/P ratio for tests 5–8 excludes sodium contributed by sulfur oxyanion salts: (1) sulfate = 6.933, (2) sulfate = 7.110, (3) sulfite = 8.593, (4) sulfite = 5.333. [c] Na/P loss calculation invalid due to suspected leaching of sodium phosphate from system crevices from a previous run that used extremely high phosphate concentrations.

Although the present experimental program was not designed to verify that threshold conditions for the reverse reaction (i.e., reaction product transformation back to ZnO) were identical to those observed for the ZnO transformation reaction, it is noted that the reversible nature of the ZnO transformation reaction was demonstrated in our previous ZnO/$NaZnPO_4$ solubility study.[1] In that study, reaction product dissolution (increases in sodium phosphate concentration) of a partially transformed ZnO bed and changes in Zn(II) ion concentration with time were monitored when the sodium phosphate concentration/temperature conditions were held below the established ZnO reaction threshold conditions.

Characterization of Reaction Product I. Individual microcrystals of the reaction product, when viewed under a stereomicroscope, appeared white and translucent. SEM photographs of representative reaction product crystals are provided in Figure 3 at magnifications between 1000 and 10 000×. These photographs reveal the crystals to have a barrellike appearance. In most instances the "barrels" have a hexagonal cross-section, a hollow center, and an l/d ratio of approximately 2/1. Crystal sizes (5–25-μm diameter) are relatively large in comparison to the unreacted zinc oxide (0.5 μm); see Figure 3b.

XRD analyses, as performed with monochromatic copper Kα X-rays, revealed that the zinc oxide decomposition products from tests 1–8 had identical crystalline lattice configurations; that is, they were the same compound. Only in test 4 were the peak intensities sufficiently strong to provide an X-ray diffraction pattern useful for reference purposes; see Table 2. A search of the JCPDS database[4] revealed that although the reaction product possessed some similarities with the α-$NaZnPO_4$ compound generated by Kolsi et al.[5] under nonhydrothermal conditions, the interplanar spacings are most consistent with the $Na(Zn_{0.8}Fe_{0.2})PO_4$ compound generated by Kabalov et al.[6] via a hydrothermal synthesis. Their reported crystal symmetry is monoclinic with unit cell lattice parameters of a = 8.668 ± 0.006, b = 8.125 ± 0.004, and c = 15.281 ± 0.001 Å; β = 90.17°. An indexing of the Table 2 X-ray diffraction pattern by means of the DICVOL computer code[7] obtained a satisfactory fit with an orthorhombic unit cell having lattice parameters a = 8.710 ±

(4) JCPDS Powder Diffraction File, International Centre for Diffraction Data, Swarthmore, PA, 1989; Sets 1–39.
(5) Kolsi, A.-W.; Erb, A.; Freundlich, W. *C. R. Acad. Sci. Paris, Ser. C* **1976**, *282*, 575.
(6) Kabalov, Yu. K.; Simonov, M. A.; Mel'nikov, O. K.; Belov, N. V. *Sov. Phys.—Dokl.* **1973**, *17*, 835.
(7) Louer, D.; Louer, M. *J. Appl. Crystallogr.* **1972**, *5*, 271.

(a) 1000X

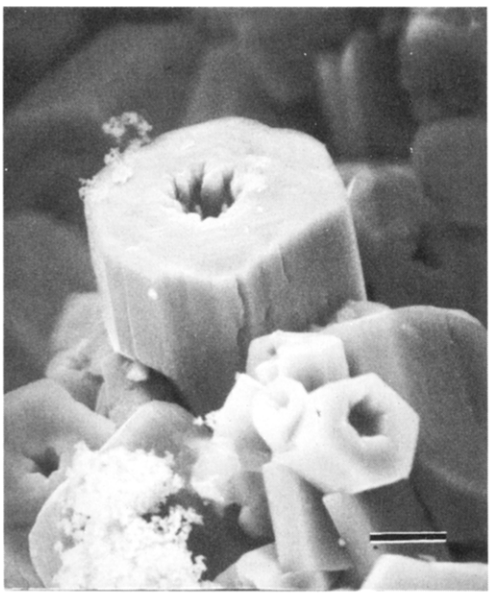

(b) 10,000X

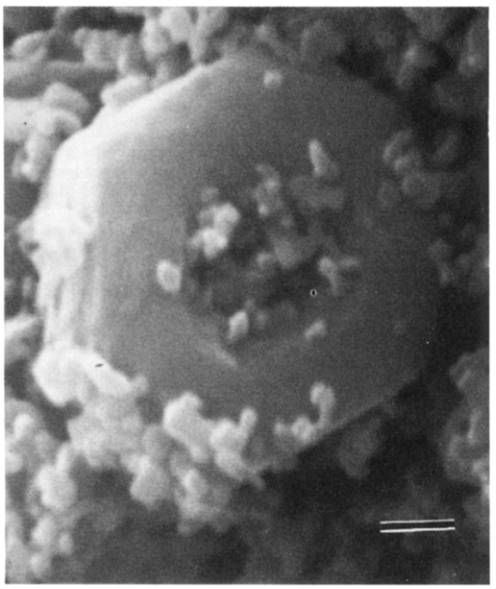

Figure 3. Scanning electron micrographs of zinc oxide–sodium phosphate reaction products. Bar length corresponds to 10 and 1 μm in (a) and (b), respectively.

0.013, b = 15.175 ± 0.010, and c = 8.027 ± 0.004 Å (i.e., β = 90°). The figure of merit for this fit (F_{31} = 4.6) is consistent with an average (absolute) discrepancy in 2θ of 0.028°.

Standard quantitative chemical analyses of the test 4 reaction product performed after digestion in nitric acid yielded

element	wt %	atom ratio to P
Na	11.10	0.94
P (as PO_4)	15.88 (49.50)	
Zn	37.19	1.11
	total 97.8	

A Zn/P atom ratio slightly in excess of unity, along with approximately 2% unaccounted for material (assumed to be oxygen), is consistent with the presence of 5–10% unreacted ZnO in the test 4 reaction cake. The absence of hydroxyl ions was inferred from the absence of an infrared absorption peak in the vicinity of 3500 ± 100 cm^{-1}, which corresponds to the expected stretching frequency of the O–H bond. This result is also consistent with the quantitative elemental results.

Assembly of the above information gives the ZnO decomposition product stoichiometry as Na/P = Zn/P = 1, or $NaZnPO_4$.

Zinc Oxide Phase Boundary II. Three additional tests were conducted using lower phosphate concentrations; see Table 3. As expected, lower phosphate concentrations led to higher reaction threshold temperatures.

Table 2. Indexed Power X-ray Diffraction Pattern of Zinc(II) Oxide-Sodium Phosphate Reaction Product

measd d spacing, Å	pattern rel int, I/I_0	reflection plane indices h	k	l	calcd d spacing, Å
5.88	6	1	0	1	5.903
4.646	35	1	2	1	4.659
4.360	65	2	0	0	4.355
		1	3	1	4.374
4.008	80	0	0	2	4.014
3.883	17	0	1	2	3.880
3.710	18	2	1	1	3.712
3.290	11	1	2	2	3.286
3.198	14	1	4	1	3.192
3.147	6	0	3	2	3.144
3.058	6	2	3	1	3.052
2.959	100	2	0	2	2.952
		1	3	2	2.958
2.863	18	2	4	0	2.860
		1	5	0	2.866
2.629	20	1	4	2	2.629
2.522	70	1	1	3	2.522
		0	2	3	2.524
2.414	31	0	6	1	2.413
2.331	7	2	4	2	2.330
		1	5	2	2.332
2.280	8	2	0	3	2.280
		1	3	3	2.283
2.252	20	2	1	3	2.255
2.182	9	2	2	3	2.184
2.117	27	2	5	2	2.116
2.007	6	0	0	4	2.007
		0	5	3	2.007
1.989	10	0	1	4	1.990
1.922	14	2	6	2	1.920
1.834	5	3	3	3	1.834
1.824	9	2	0	4	1.823
		1	3	4	1.824
		2	5	3	1.823
1.676	14	0	5	4	1.674
1.650	5	3	0	4	1.651
		4	2	3	1.649
		3	5	3	1.651
		4	6	0	1.650
		0	9	1	1.650
1.573	6	1	1	5	1.570
		0	2	5	1.571
		0	6	4	1.572
		2	9	0	1.572
1.528	14	1	9	2	1.530
1.508	23	2	0	5	1.506
		1	3	5	1.507
		4	7	1	1.509
1.460	16	5	0	3	1.460
		1	4	5	1.458

Table 3. Additional Zinc(II) Oxide Reaction Thresholds

test	baseline phosphate	baseline Na/P	threshold temp, K	final phosphate	final Na/P	indicated Na/P loss
9	2.864	2.164	494	2.611	2.538	−1.7
10	2.611	2.453	528	2.316	2.750	0.1
11	1.885	2.150	481	1.485	2.735	0.0

Table 4. Comparison of Powder X-ray Diffraction Patterns of Second Zinc(II) Oxide–Sodium Phosphate Reaction Product and Synthetic Tarbuttite

synthetic tarbuttite[8]		Composite Pattern of Tests 9–11	
d spacing, Å	rel int I/I_0	*d* spacing, Å	rel int I/I_0
6.18	100	6.14	35
5.37	15	5.42	25
4.59	12	4.58	20
3.69	45	3.68	85
3.266	70	3.26	90
2.971	40	2.97	35
2.876	45	*a*	*a*
2.771	40	*a*	*a*
2.928	15	*a*	*a*
2.471	50	*a*	*a*
2.416	30	2.43	20
2.355	15	2.354	40
2.055	30	2.054	25

[a] Obscured by overlap with ZnO line.

However, the inferred reaction product composition differed from the preceding results in that no sodium losses were observed. The reaction appeared to be self-limiting, undoubtedly due to the relatively large increases in solution Na/P ratios created by the reaction. That is, the higher Na/P ratios created a test environment where the ZnO phase was once again stable.

Characterization of Reaction Product II. The extremely small amounts of phosphate reacted in this three run series (average = 0.3 mmol of P) made a positive identification by bulk analysis very difficult. XRD analyses of selected regions of the ZnO "cakes" enriched with reaction products, however, confirmed that the reaction product's major lines were coincident with the major (i.e., $I/I_0 > 10\%$) lines of synthetic tarbuttite;[8] see Table 4.

Chemical analyses of individual microcrystals of the reaction product were performed using a JEOL Model JXA-8600 electron microprobe operated at 15 kV. The results indicated the following atomic ratios: Zn/P = 2.2, O/P = 4.5, with estimated uncertainties of ±15% (1σ). Only trace levels of sodium were detected, i.e., <5%. Therefore, the above analyses confirm that the second ZnO decomposition product is tarbuttite, $Zn_2(OH)PO_4$.

Discussion

The present experiments demonstrate that zinc(II) oxide was decomposed by relatively dilute sodium phosphate solutions. On the basis of observed reaction product stoichiometries, two ZnO decomposition reaction equilibria were isolated:

$$ZnO(s) + Na^+ + H_2PO_4^- \rightleftarrows NaZnPO_4(s) + H_2O \quad (2)$$

or

$$2ZnO(s) + H_3PO_4(aq) \rightleftarrows Zn_2(OH)PO_4(s) + H_2O \quad (3)$$

The existence of other ZnO decomposition products, such as $NaZn_2(PO_4)(HPO_4)$ and $Na_2Zn(OH)PO_4$, which have been hydrothermally synthesized in the respective phosphoric acid[9] and trisodium phosphate[10] solutions, has been ruled out because of their nonrepresentative Na/P ratios.

Equilibrium constants for eqs 2 and 3 were defined by

$$K_{(2)} = \frac{a_{NaZnPO_4}a_{H_2O}}{a_{ZnO}a_{Na^+}a_{H_2PO_4^-}} \quad (4)$$

$$K_{(3)} = \frac{a_{Zn_2(OH)PO_4}a_{H_2O}}{a_{ZnO}^2a_{H_3PO_4}} \quad (5)$$

In the usual manner, activities (a_i) of water and all solid phases were taken to be unity, whereas ionic activity coefficients (γ_i) were used to relate ionic concentrations [C_i] in molality units to thermodynamic activities. Marshall and Jones[11] have shown that an extended Debye–Hückel equation of the form

$$\log \gamma_i = -Z_i^2 S\sqrt{I}/(1 + A\sqrt{I}) \quad (6)$$

with $A = 1.5$ gives reasonable approximations at temperatures in the range 400–500 K for ionic strengths ($I = 0.5\sum C_iZ_i^2$) typical of our tests. In eq 6, Z_i is the ionic charge number and S is the limiting Debye–Hückel slope (0.51 at 298 K).[12]

Combining eqs 2–6 yields

$$\log K_{(2)} = \log Q_{(2)} + 2S\sqrt{I}/(1 + 1.5\sqrt{I}) \quad (7)$$

where

$$\log Q_{(2)} = -\log [Na^+][H_2PO_4^-]$$

$$\log K_{(3)} = -\log [H_3PO_4] \quad (8)$$

An ion electroneutrality balance, which accounted for changes in water,[12] phosphate ion,[13,14] and sulfur oxyanion[15,16] dissociation behavior with temperature and ionic strength, was then employed to determine $H_2PO_4^-$ and H_3PO_4(aq) concentrations at the Tables 1 and 3 threshold conditions. For the most general case, with sodium phosphate and sodium sulfite present, the balance is

$$[H^+] + [Na^+] = 3[PO_4^{3-}] + 2[HPO_4^{2-}] + [H_2PO_4^-] + 2[SO_3^{2-}] + [HSO_3^-] + [OH^-] \quad (9)$$

This balance was converted to a mathematical equation by introducing the following equilibrium constants defined in terms of thermodynamic activities (parentheses):

$$K_w = (H^+)(OH^-) \qquad K_1 = \frac{(H_2PO_4^-)}{(H_3PO_4(aq))(OH^-)}$$

$$K_I = \frac{(H^+)(HSO_3^-)}{(H_2SO_3(aq))} \qquad K_2 = \frac{(HPO_4^{2-})}{(H_2PO_4^-)(OH^-)} \quad (10)$$

$$K_{II} = \frac{(H^+)(SO_3^{2-})}{(HSO_3^-)} \qquad K_3 = \frac{(PO_4^{3-})}{(HPO_4^{2-})(OH^-)}$$

with $\log K_i = b_1/T + b_2 + b_3 \ln T + b_4T + b_5/T^2$.

(8) Milnes, A. R.; Hill, R. J. *Neues Jahrb. Mineral., Monatsh.* **1977**, *1*, 25.
(9) Kabalov, Yu. K.; Simonov, M. A.; Yakubovich, O. V.; Belov, N. V. *Sov. Phys.—Dokl.* **1974**, *18*, 627.
(10) Kabalov, Yu. K.; Simonov, M. A.; Belov, N. V. *Sov. Phys.—Dokl.* **1972**, *17*, 77.
(11) Marshall, W. L.; Jones, E. V. *J. Phys. Chem.* **1966**, *70*, 4028.
(12) Sweeton, F. H.; Mesmer, R. E.; Baes, C. F. *J. Solut. Chem.* **1974**, *3*, 191.
(13) Mesmer, R. E.; Baes, C. F. *J. Solut. Chem.* **1974**, *3*, 307.
(14) Treloar, N. C. Central Electricity Research Laboratory Report RD/L/N 270/73, 1973.

Table 5. Dissociation Behavior of Selected Compounds

K_i	b_1	b_2	b_3	b_4	b_5	ref
K_w	31 286.0	−606.522	94.9734	−0.097 611	−2 710 870	Sweeton et al.[12]
K_1	17 655.8	−253.198	39.4277	−0.032 540 5	−810 134	Mesmer and Baes[13]
K_2	17 156.9	−246.045	37.7345	−0.032 208 2	−897 579	Mesmer and Baes[13]
K_3	−106.51	7.1340		−0.017 459		Treloar[14]
K_I	−1424.4	10.192		−0.024 982		Khodakovskii et al.[15]
K_{II}	−1629.1	5.733		−0.025 214		Khodakovskii et al.[15]
K_I (sulfate)	593 089	−8550.82	1343.462	−1.019 062	−43 593 400	Oscarson et al.[16]
K_{II} (sulfate)	119 452	−1974.81	305.682	−0.275 677	−7 715 600	Oscarson et al.[16]
K_{IP}[a] (sulfate)	9 303	−266.96	38.202	−0.057 73	−462 000	Oscarson et al.[16]

[a] log K for dissociation of ion pair, $NaSO_4^-$. Note that inclusion of this species in eq 9 requires modification of eq 11 prior to calculating reaction threshold values for tests 5 and 6.

Table 6. Solution Chemistry Values Used To Define the $ZnO/NaZnPO_4$ and $ZnO/Zn_2(OH)PO_4$ Phase Boundaries

test	$[Na^+]$, m	$[H_2PO_4^-]$, m	log Q_1	I	S	ΔG, kJ/mol
1	1.312×10^{-2}	5.815×10^{-4}	5.1173	0.01861	0.7640	−46.08
2	1.635×10^{-2}	5.128×10^{-4}	5.0767	0.02243	0.8374	−48.73
3	1.763×10^{-2}	2.851×10^{-4}	5.2992	0.02369	0.8057	−49.60
4	2.418×10^{-1}	2.188×10^{-5}	5.2765	0.3711	0.5798	−38.71
5	2.730×10^{-2}	1.258×10^{-4}	5.4642	0.04034	0.6424	−43.03
6	2.889×10^{-2}	2.179×10^{-4}	5.2010	0.04177	0.7355	−46.06
7	3.212×10^{-2}	1.124×10^{-4}	5.4424	0.04314	0.7265	−47.67
8	2.419×10^{-2}	1.391×10^{-4}	5.4730	0.03123	0.7640	−49.53
			$[H_3PO_4]$			
9	6.198×10^{-3}	8.260×10^{-4}	8.795×10^{-9}	0.00824		−76.18
10	6.405×10^{-3}	9.204×10^{-4}	1.320×10^{-8}	0.00810		−79.64
11	4.053×10^{-3}	5.868×10^{-4}	7.052×10^{-9}	0.00535		−75.06

The above parameters are tabulated in Table 5. Upon substitution of the eq 10 dissociation constants into eq 9 and applying the known levels of total dissolved sulfite, $[m_s]$, and phosphate, $[m_p]$ (and its associated sodium-to-phosphate molar ratio, y), the neutrality balance reduced to an algebraic equation in terms of the unknown $[H^+]$, i.e., x:

$$x + (y-3)m_p = \frac{-m_p\left[1+\left(2-\frac{3x}{K_wK_1}\right)\frac{x}{K_wK_2}\right]\frac{x}{K_wK_3}}{1+\left[1+\left(1+\frac{x}{K_wK_1}\right)\frac{x}{K_wK_2}\right]\frac{x}{K_wK_3}} \frac{-m_s\left(1+\frac{2x}{K_I}\right)\frac{x}{K_{II}}}{1+\left(1+\frac{x}{K_I}\right)\frac{x}{K_{II}}} + \frac{K_w}{x} \quad (11)$$

Equation 11 represents a seventh-order polynomial equation in terms of the unknown, x, and was solved by a Newton–Raphson iteration procedure. The calculated reaction threshold values for $[H^+]$, along with those for $[H_2PO_4^-]$ and $[H_3PO_4(aq)]$, are given in Table 6. It is noted that measured and calculated pH values (at room temperature) for all baseline test solutions agreed to within the reproducibility of the measurements (±0.05). All ΔG values reported in the final column of Table 6 were determined from the expression

$$\Delta G_i = -RT \ln K_i \quad (12)$$

Least-squares fits of the Table 6 results (see Figures 4 and 5) yield

$ZnO/NaZnPO_4$:

$$\Delta G \text{ (kJ/mol)} = -8522 \pm 5395 - (86.06 \pm 12.28)T \quad (13)$$

$ZnO/Zn_2(OH)PO_4$:

$$\Delta G \text{ (kJ/mol)} = -27640 \pm 1698 - (98.44 \pm 3.39)T \quad (14)$$

Equation 13 provides free energy changes for eq 2 with an estimated standard deviation of ±1.15 kJ/mol over the temperature range 350–490 K. An independent estimate of the eq 2 equilibrium, based on our previous ZnO solubility study,[1] is plotted for comparison purposes in Figure 4. Given the precision of the latter estimate (1σ = ±3.0 kJ/mol), the observed 2 kJ/mol difference between the two correlations is not significant. Combination of the above results with previously established thermodynamic properties yields the summary presented in Table 7.

The observed susceptibility of ZnO to hydrothermal degradation in alkaline sodium phosphate solutions has led to the precipitation of sodium–zinc(II) phosphate phases that are unique with respect to neighboring divalent transition metal ions: Na^+ and OH^- have not precipitated concurrently. That is, $Na_2Zn(OH)PO_4$ was *not* observed. Although the latter compound has been hydrothermally formed in trisodium phosphate and sodium sulfate solutions,[10] the present results confirm that $NaZnPO_4$ is the preferred zinc(II) oxide decomposition product at lower solution alkalinities.

It is noteworthy that the orthorhombic structure of $NaZnPO_4$ is virtually identical to that possessed by

(15) Khodakovskii, I. L.; Ryzhenko, B. N.; Naumaov, G. B. *Geochem. Int.* **1968**, *5*, 1200.
(16) Oscarson, J. L.; Izatt, R. M.; Brown, P. R.; Pawlak, Z.; Gillespie, S. E.; Christensen, J. J. *J. Solut. Chem.* **1988**, *17*, 841.
(17) Criss, C. M.; Cobble, J. W. *J. Am. Chem. Soc.* **1964**, *86*, 5390.
(18) Abraham, M. H.; Marcus, Y. *J. Chem. Soc., Faraday Trans. 1* **1986**, *82*, 3255.
(19) Wagman, D. D.; Evans, W. H.; Parker, V. B.; Schumm, R. H.; Halow, I.; Bailey, S. M.; Churney, K. L.; Nuttall, R. L. *J. Phys. Chem. Ref. Data* **1982**, *11*, Suppl. 2.
(20) Khodakovskii, I. L.; Elkin, A. E. *Geokhimiya* **1975**, *10*, 1490.
(21) Kubaschewski, O.; Alcock, C. B. *Metallurgical Thermochemistry*; Pergamon Press: Oxford, 1983.
(22) Larson, J. W.; Zeeb, K. G.; Hepler, L. G. *Can. J. Chem.* **1982**, *60*, 2141.
(23) Vieillard, P.; Tardy, Y. In *Phosphate Minerals*; Nriagu, J. O., Moore, P. B., Eds.; Springer-Verlag: Berlin, 1984; Chapter 4.
(24) Magalhaes, M. C. F.; deJesus, J. P.; Williams, P. A. *Mineral. Mag.* **1986**, *50*, 33.

Table 7. Thermochemical Parameters for Selected Species in the $ZnO-Na_2O-P_2O_5-H_2O$ System at 298.15 K

species	$C_p°(298)$, J mol^{-1} K^{-1}	$S°(298)$, J mol^{-1} K^{-1}	$\Delta H_f°(298)$, kJ mol^{-1}	$\Delta G_f°(298)$, kJ mol^{-1}	ref
$H^+(aq)$[a]	−71 ± 1	−22.2	0	0	17, 18
$Na^+(aq)$	−24.6	36.8	−240.12	−261.91	19
$Zn^{2+}(aq)$	−164	−154.8 ± 1.3	−153.64 ± 0.42	−147.23	18, 20
$H_2(g)$	28.83	130.58 ± 0.08	0	0	21
$O_2(g)$	29.37	205.02 ± 0.4	0	0	21
H_2O	75.31	69.96 ± 0.08	−285.85 ± 0.04	−237.19 ± 0.04	21
$PO_4^{3-}(aq)$	−283 ± 20	−153.6	−1277.4	−1018.8	19, 22
$HPO_4^{2-}(aq)$	−112 ± 4	−32.6	−1305.5	−1089.7	14, 22
$H_2PO_4^-(aq)$	37 ± 4	72.4	−1308.8	−1130.8	13, 22
$H_3PO_4(aq)$	94 ± 4	119.8	−1300.2	−1143.0	13, 22
Na(s)	28.24	51.21	0	0	19
P(s)	23.84	41.09	0	0	19
Zn(s)	23.40	41.63 ± 0.21	0	0	21
ξ-$Zn(OH)_2(s)$	72.4	76.99 ± 0.21	−645.47	−555.93 ± 0.21	20
ZnO(s)	40.25	43.64 ± 0.42	−350.83 ± 0.21	−320.91 ± 0.25	21
α-$Zn_3(PO_4)_2{\cdot}4H_2O(s)$		372.7	−4102.0	−3628.9	23
$Zn_3(PO_4)_2{\cdot}2H_2O(s)$		243.0	−3516.3	−3143.5	23
$Zn_3(PO_4)_2{\cdot}H_2O(s)$		184.3	−3211.7	−2890.9	23
$Zn_3(PO_4)_2(s)$		134.3	−2899.6	−2633.4	23
$Zn_2(OH)PO_4{\cdot}1.5H_2O(s)$				−1982.4 ± 3.1	24
$Zn_2(OH)PO_4(s)$		235.9[b]	−1743.6	−1604.6	this work
				−1632.1 ± 4.0	24
$NaZnPO_4(s)$	150.3[b]	169.0	−1622.4	−1510.6	1, this work

[a] Tabulated $C_p°$ and $S°$ values differ from the usual convention of zero due to conversion to an absolute scale of ionic properties. [b] Mean values over temperature range of this study.

Table 8. Estimated Reaction Thresholds for Zinc(II) Oxide Decomposition in the $ZnO-P_2O_5-H_2O$ Ternary Oxide System at 298.15 K

decomposition reaction	$\Delta G°$, kJ/mol	log $[H_3PO_4(aq)]$, mol/kg
$2ZnO(s) + H_3PO_4(aq) + {}^1/_2H_2O \rightleftarrows Zn_2(OH)PO_4{\cdot}1.5H_2O(s)$	−78.94	−13.831
$2ZnO(s) + H_3PO_4(aq) \rightleftarrows Zn_2(OH)PO_4(s) + H_2O$	−84.42	−14.791
$3ZnO(s) + 2H_3PO_4(aq) + H_2O \rightleftarrows \alpha$-$Zn_3(PO_4)_2{\cdot}4H_2O(s)$	−142.89	−12.518
$3ZnO(s) + 2H_3PO_4(aq) \rightleftarrows Zn_3(PO_4)_2{\cdot}2H_2O + H_2O$	−131.65	−11.533
$3ZnO(s) + 2H_3PO_4(aq) \rightleftarrows Zn_3(PO_4)_2{\cdot}H_2O + 2H_2O$	−116.43	−10.200

beryllonite ($NaBePO_4$):[25] $a = 8.16$, $b = 14.08$, and $c = 7.79$ Å; the lower lattice constants being caused by the smaller size of the Be(II) ion relative to the Zn(II) ion. On the other hand, the structural similarity between $NaZnPO_4$ and the $Na(Zn_{0.8}Fe_{0.2})PO_4$ compound reported by Kabalov et al.[6] indicates that zinc(II) oxide decomposition in the presence of solubilized Fe(II) ions may lead to crystallization of an "impure" sodium zinc phosphate precipitate that represents a solid solution of Zn(II) and Fe(II) ions – $Na(Zn_{1-x}Fe_x)PO_4$. The incorporation of Fe(II), however, may cause slight lattice distortions which lead to a monoclinic cell, i.e., 90 → 90.2°.

To more fully interpret the significance of formation of a sodium-less ZnO decomposition product in alkaline sodium phosphate solutions having Na/P ≥ 2.0, a comparison of equilibrium constants associated with the formation of some zinc phosphate minerals expected to exist in the $ZnO-P_2O_5-H_2O$ ternary oxide system is given in Table 8. These estimates were derived from recent room temperature solubility studies for α-hopeite,[26] tarbuttite,[24] and spencerite.[24] On the basis of the Table 7 compilation, $\Delta G°$ estimates (hence equilibrium constants) were obtained for potential ZnO decomposition reactions. As expected, a $Zn_3(PO_4)_2$ solid having four waters of hydration is the stable zinc phosphate phase at room temperature, and progressive dehydration to two, one, and zero waters of hydration may be expected as temperature increases. On the other hand, an anhydrous $Zn_2(OH)PO_4$ solid is expected to be thermodynamically stable with respect to the hydrated form (spencerite) at room temperature.[24] The calculated threshold concentrations of $H_3PO_4(aq)$ required to initiate these reactions are compared in Table 8. This comparison reveals that the tarbuttite formation reaction requires the *lowest* concentrations of $H_3PO_4(aq)$ in order to procede. Since the initial solutions for tests 9–11 had room-temperature log $[H_3PO_4(aq)]$ values that ranged between −14.4 and −15.5 and were higher than in the first eight runs, it is seen that temperature increases were sufficient to cause the ZnO/$Zn_2(OH)PO_4$ phase boundary to be crossed.

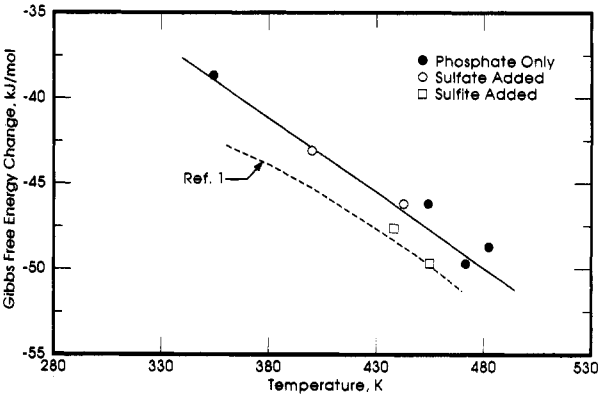

Figure 4. Free energy changes determined for zincite transformation to sodium–zinc phosphate in alkaline sodium phosphate solutions.

An inconsistency exists with regard to the ZnO/$Zn_2(OH)PO_4$ phase boundary, since the present three high-temperature points do not extrapolate linearly to the implied room temperature estimate[24] (see Figure 5). It is noted that the initial (i.e., room temperature) $H_3PO_4(aq)$

(25) Golovastikov, N. I. *Sov. Phys.—Crystallogr.* **1962**, *6*, 733.
(26) Nriagu, J. O. *Geochim. Cosmochim. Acta* **1973**, *37*, 2357.

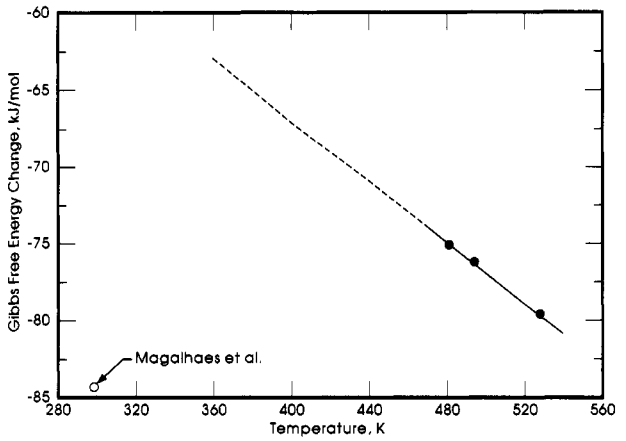

Figure 5. Free energy changes determined for zincite transformation to dizinc hydroxyphosphate (tarbuttite) in alkaline sodium phosphate solutions.

concentration used in test 11 was greater than the implied H_3PO_4(aq) threshold concentration for eq 3, based on the results of Magalhaes et al.[24] Therefore, the true $\Delta G°$ value for eq 3 must be greater than −81.98 kJ/mol. Considering the reported uncertainty in $\Delta G_f°$ for tarbuttite formation (±4.0 kJ/mol per Table 7) and invoking a 2σ limit, allows an upper limit of $\Delta G° = -76.4$ kJ/mol to be derived for eq 3 using the results of Magalhaes et al.[24] This estimate differs by ~19 kJ/mol from one based on extrapolation of the eq 3 equilibrium via eq 14: $\Delta G° = -57.0$ kJ/mol. Although some of the observed discrepancy may be due to a heat capacity effect (i.e., curvature in the ΔG versus T correlation), the absence of heat capacity data for $Zn_2(OH)PO_4$ does not allow this contribution to be estimated. Therefore, the presently extrapolated thermochemical parameters for tarbuttite are considered tentative, pending completion of a ZnO phase stability study in sodium phosphate solutions having Na/P ≤ 2.

Acknowledgment. We are indebted to the following individuals who contributed professional assistance: P. C. Sander for X-ray diffraction analyses; Dr. J. J. Cheung for infrared spectroscopy; G. M. Neugebauer for scanning electron microscopy; and V. P. Nordstrom for electron microprobe quantitative chemical analyses. The Knolls Atomic Power Laboratory is operated for the U.S. Department of Energy by KAPL, Inc., a wholly owned subsidiary of the Martin Marietta Corp., under Contract DE-AC12-76-SN00052.